Multi surface retracker for swath processing of interferometric radar altimetry

Multi surface retracker for swath processing of interferometric radar altimetry

Albert Garcia-Mondéjar, Noel Gourmelen, Maria José Escorihuela, Mònica Roca, Andrew Shepherd, Stephen Plummer

***Abstract*— Swath mode processing of CryoSat-2 SARIn mode has been used to monitor elevation of areas with complex topography such as over ice sheet and ice cap margins. Swath processing relies on an accurate measure of the angle of arrival of the measured echo and therefore requires custom strategies in order to resolve the ambiguous phase measurement. In mountainous regions of complex terrain, it may be necessary to apply different phase ambiguities across a waveform record when returns come from different scatters distributed perpendicularly to the CryoSat-2 ground tracks. In this paper, we present modifications to the conventional swath processing method whereby a multi-surface retracker is first applied to the record in order to identify potential different scattering surfaces. Phase ambiguity is then independently resolved for each of these sub-surfaces. The improvements with this new method over the Karakoram glaciers are a 10% increase in the number of measurements with improvements of almost 50% for individual glaciers and a reduction in the median absolute deviation of the elevations from 20.18 to 14.69 metres.**

***Index Terms*— Mountain Glaciers, CryoSat-2, SAR Interferometry, Swath Processing**

I. Introduction

Earth's land ice, comprising the Greenland and Antarctic ice sheets, ice caps and mountain glaciers, is losing mass and is estimated to have contributed 31 mm towards global sea-level rise since 1992 [1][2]. The role of glaciers in current sea-level budgets is significant and is expected to continue over the next century and beyond [2], particularly in the Arctic where mean annual surface temperatures have been increasing twice as fast as the global average [9]. Glaciers in High Mountain Asia (more than 110,000 km^2 of glacier area) have experienced losses in recent decades, but the region is sparsely observed and uncertainties are generally large [3][4][5][6]. However, mountain glaciers have been studied less than polar ice caps due to the limited performance of altimetry over complex topography [7][8]. Since 2010, the Synthetic Interferometric Radar Altimeter (SIRAL) onboard the European Space Agency (ESA) radar altimetry CryoSat-2 mission has been collecting ice elevation measurements over glaciers and ice caps. Its Synthetic Aperture Radar Interferometric (SARIn) instrument mode reduces the size of the footprint along-track and locates the across-track origin of a surface reflector in the presence of a slope. This offers new avenues for the measurement of regions marked by complex topography [10][11]. Recently, data from the SARIn mode have been used to infer elevation from the point of closest approach (POCA) to additional observations with an approach known as "swath processing". This processing technique allows to form denser and statistically robust time series of elevation change improving the temporal resolution by a factor of 5 compared with the POCA method. It enables the study of key processes that underlie current changes in the cryosphere [12][13][14] in particular for ice caps and glaciers.

The swath processing method relies on selecting the measurements using quality criteria of power, coherence and surface slopes. The algorithm then needs to correctly unwrap the measurements to ensure accurate vertical and planimetric geolocation; the correct 2π modulus to apply to the raw phase measurement is generally chosen based on phase continuity and a minimization scheme on a waveform by waveform basis. These routine approaches make the assumption that the surface terrain is homogeneous within the beam-limited footprint area, an assumption that is not applicable in most mountainous regions where the surface topography is complex. In these regions, a given waveform can contain echoes from an interferometric phase greater than π, which current approaches cannot properly deal with. The solution proposed in this paper, the Multi Swath processor, is an adaptation of the conventional swath processor with an additional preliminary step to identify the multiple reflections that have been received on a single record. These reflections can then be treated independently during unwrapping.

II. Region Of Interest, Data and Methods

A. Region Of Interest

The Karakoram is a large mountain range spanning the borders of Pakistan, India, and China. It is home to the four most closely located peaks over 8000 m in height on earth: K2, the second highest peak in the world at 8,611 m, Gasherbrum I, Broad Peak and Gasherbrum II. It is also the most heavily glaciated part of the world outside the polar regions. Due to its challenging topography, the glaciers in this area have been selected to test the swath processing improvements. A map of the region with the distribution of the glaciers is shown in Figure 1 using glacier masks from the Global Land Ice Measurements from Space (GLIMS) database [15]. The orientation of the glaciers is an additional complexity under test because the swath processing is supposed to work better when the slope gradient is perpendicular to the ground tracks.

A. Garcia-Mondéjar, M.J. Escorihuela and M. Roca are with isardSAT Ltd., The Surrey Technology Centre, GU2 7YG, Guildford, United Kingdom.

N. Gourmelen is with School of GeoSciences, University of Edinburgh, Drummond Street, Edinburgh, United Kingdom and IPGS UMR 7516, Université de Strasbourg, CNRS, Strasbourg, France

A. Shepherd is with Centre for Polar Observation and Modelling, School of Earth and Environment, University of Leeds, Woodhouse Lane, Leeds LS2 9JT, United Kingdom

S. Plummer is with European Space Agency Climate Office, Fermi Avenue, Harwell Campus, Didcot, OX11 0FD Didcot, United Kingdom

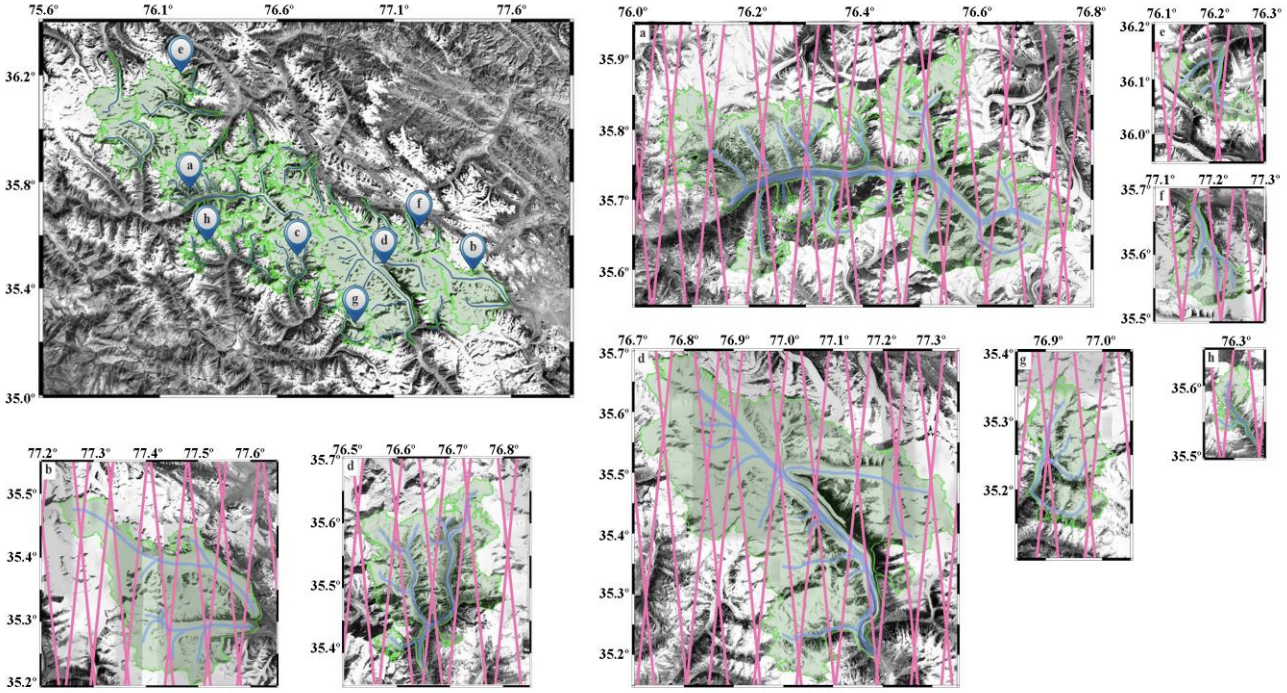

Figure 1: Top left map shows an overview of the Karakoram region, with the glaciers and tributaries trajectories in blue, the glaciers masks from GLIMS in green and a background image from Google Earth in black and white. A closer look into the most relevant glaciers of this study is shown as follows: a-Baltoro b-Rimo, c-Siachin, d-Siachen, e-G076196E36156N, f-Nagir, g-Bilafond and h-Masherbrum. CryoSat-2 tracks are shown in pink.

B. Data

The CryoSat-2 SARIn Baseline C L1b files acquired between 2010 and 2012 have been processed with the conventional swath processor [13] and a modified version of it, named the Multi Swath processor, which includes the new multi surface retracker methods described in this paper. All the CryoSat-2 data needed were delivered by ESA through the EOPI (Earth Observation Principal Investigator) portal. The SPOT5 DEM (Digital Elevation Model created from SPOT5 satellite images) was selected as the reference DEM in the phase unwrapping step and as a quality control as it was the closest in time (SPOT5-2011, ASTER-2008, STRM-2000) [4] to the CryoSat-2 datasets analysed (2010-2012). Finally, the glacier masks were obtained from the Global Land Ice Measurements from Space (GLIMS) Glacier Database (www.glims.org RGI v6.0).

C. Methods - Multi Swath Processor

The differences between the Multi Swath processor and the conventional processor are split into two blocks. The first is a preliminary step performed before the swath processing in order to partition the L1b record into sections and the second is to perform swath processing with modified configuration parameters (the coherence threshold, the phase unwrapping limit and the outlier rejection threshold).

1) Multi Surface retracker

The multi surface retracker is in charge of splitting the multi-looked SARIn waveforms into segments, enabling them to be processed independently as they may come from different angles of arrival. The coherence computed in the L1b product is used to identify regions with coherence lower than a threshold and of a longer than 3 samples. The retained sections are partitioned by these gaps and the data within the gaps are discarded. After that, the number of retained sections is counted

The steps of the retracker that allow the different surfaces, that the echo is composed of, to be identified are:

1. Identify samples with coherence higher than coherence threshold.
2. Use gaps longer than 3 samples to split the waveform in the corresponding segments.
3. Scale the power waveforms from counts to decibels (dB) by applying the echo scale factor from the L1b product.
4. Check if the maximum power of each surface is higher than a power threshold (-170 dB)

2) Swath interferometric altimetry

Three configuration parameters within the conventional processor have been reassessed: the coherence threshold, the phase unwrapping limit and the outlier rejection threshold. The coherence threshold has been relaxed from the 0.8 value used in the processing of polar regions to 0.6. This increases the number of elevation measurements in the swaths but the overall performance needs to be compared to see if they are degraded or not.

The global phase correction ($\pm 2\pi \cdot N$) limits have been increased from N=2 to N=3 in order to retrieve targets in the far ranges (from 34 to 47km) in the across track direction.

Finally, the threshold to filter out elevations with a DEM difference greater than 50 metres has been also increased to 150 metres. Surge events can produce fast and large (about tens of metres in a matter of a few days) elevation changes that should not be filtered out.

III. Analysis and Results

A. Multi Surface identification

The complex signal backscattered from a mountain region can be observed in the L1b data shown in Figure 2. The sudden changes in power, coherence and angle of arrival are clear, as is the

segmentation into six different sections.

The process of selecting the best phase wrapping factor is an iterative loop that consists of computing the elevations and locations for each ambiguous region for each different selected section of the waveforms and evaluating them against the DEM used as a reference in that particular location (Figure 3, top subplot) [13]. The value of the N that gives the lowest deviation in elevation is used to compute the elevations (Figure 3, bottom plot). Relaxing the coherence threshold increases the number of points retrieved but the higher noise of the angle of arrival may worsen the precision of the measurements. In the conventional swath processing, this N was a common value for each L1b record, preventing the possibility of having reflections from more than one ambiguous region.

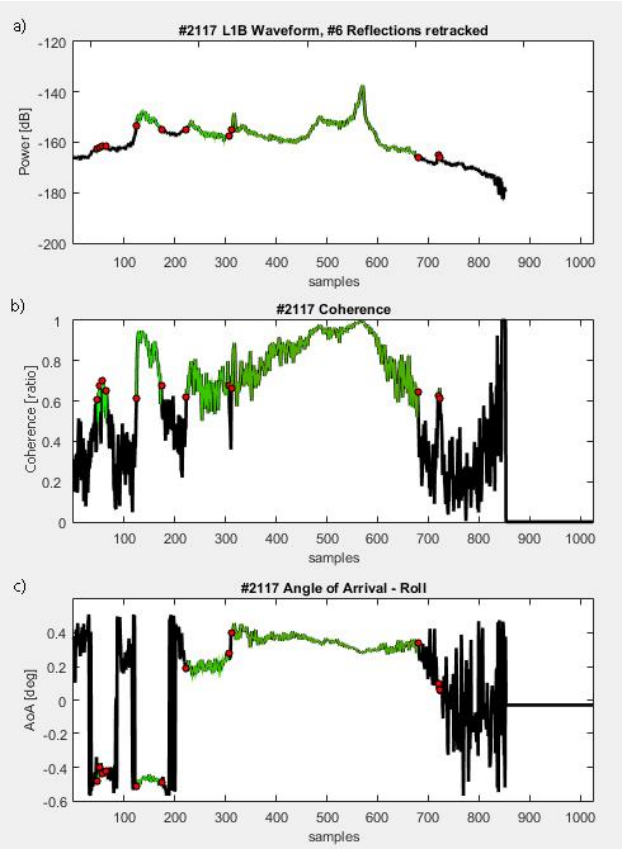

Figure 2 Example of L1b data SIR_SIN_1B_20100717T194535 file and the process of identifying the multiple echoes for a coherence > 0.6. The subplots of a) the waveform, b) the coherence and c) the angle of arrival are depicted, highlighting in green the selected sections computed by the Multi Surface retracker. The red bullets indicate the start and end sample of each segment.

B. Results of configuration parameter assessment

The parameters chosen to evaluate the quality of the results are the mean value of the difference between the elevation measurements and the reference DEM (DEM Diff) and the median absolute deviation (MAD) [13] which measures the dispersion of the elevation biases.

$$MAD = median\ (DEM\ Diff - median\ (DEM\ Diff)) \quad (1)$$

Relaxing the coherence threshold down to 0.6 allows the retrieval of more elevation measurements. In Figure 2 six different reflections are identified whereas only two would be retrieved with the 0.8 threshold, with fewer points on them. The advantage of including the number of points to increase the coverage has to be balanced against the performance as their quality is lower. The impact of relaxing the outlier rejection threshold from 50 to 150 metres is a 22% increasing in the number of elevations retrieved with a degradation in the DEM Diff and the MAD of 1.27 and 1.77 metres respectively. The effect of increasing the off nadir margins to bring just 38 new measurements without increasing or decreasing the overall results.

For the glaciers analysed, the combined impact of the reassessed configuration parameters is an increase of 404% in the number of measurements and a slightly degradation in the DEM Diff and the MAD changing from 5.77 to 7.57 metres (+1.8 metres) and from 9.46 to 14.69 (+4.14) metres respectively. The large increase in observations, in particular, for glaciers with few measurements previously, justifies these small changes in performance (see section C below) and increases the chances of generating elevation and volume time series for the first time in this region using altimetry measurements.

C. Conventional vs Multi Swath results

The CryoSat-2 L1b data have been processed with both the conventional swath and the Multi Swath processor using the same reassessed configuration parameters. For each of the glacier regions, the retrieved elevations have been evaluated and the results from both processors have been compared. Table 1 shows the results corresponding to the number of measurements retrieved for each glacier and the overall computation. Overall, the Multi Swath processor retrieves 10% more measurements with significant improvements in G076196E36156N (+49%) Bilafond (42%), Masherbrum (37%) and Nagir (+32%) glaciers. These improvements are hypothesized to be due to the northward orientation of the main glacier its tributaries. Figure 4 shows the elevations retrieved with the differences between the conventional and Multi Swath retrievals for the Baltoro and Nagir glaciers. The improvement in the number of new elevations enables new regions to be mapped that were not monitored in the conventional processing. The limitation in the conventional swath of having a single global phase correction per record does not allow the measurement simultaneously of echoes from surfaces separated more than one ambiguous region in the across track direction. This limitation is solved with the multi swath approach and more measurements are retrieved in glaciers with tributaries parallel to the CryoSat-2 ground tracks.

In terms of precision (MAD) and accuracy (DEM Diff), the results show a common improvement in the precision in all the glaciers but the accuracy is not improved uniformly. The improvement in the MAD in the Multi Swath processor is 5.49 metres. Table 2 shows the results after grouping glaciers by their slope gradient orientation showing that Multi Swath processing improves the DEM Diff by 1.31 metres when the glaciers are north/southward.

IV. Conclusion

The swath processing technique is key to getting the most out of the SARIn mode from CryoSat-2. We have described an approach to split the returns from a single record into multiple segments. This approach helps to improve the echo relocation and increases the number of elevation measurements that can be derived when the terrain geometry is complex and leading to echoes from targets located at different ambiguous ranges. The reassessed configuration parameters allowed an increase in the number of retrievals, by 10% on average and up to 50% in the most favourable glacier, with and a reduction in the median absolute deviation of the elevations from 20.18 to 14.69 metres.

Further work needs to be done to perform temporal series after the

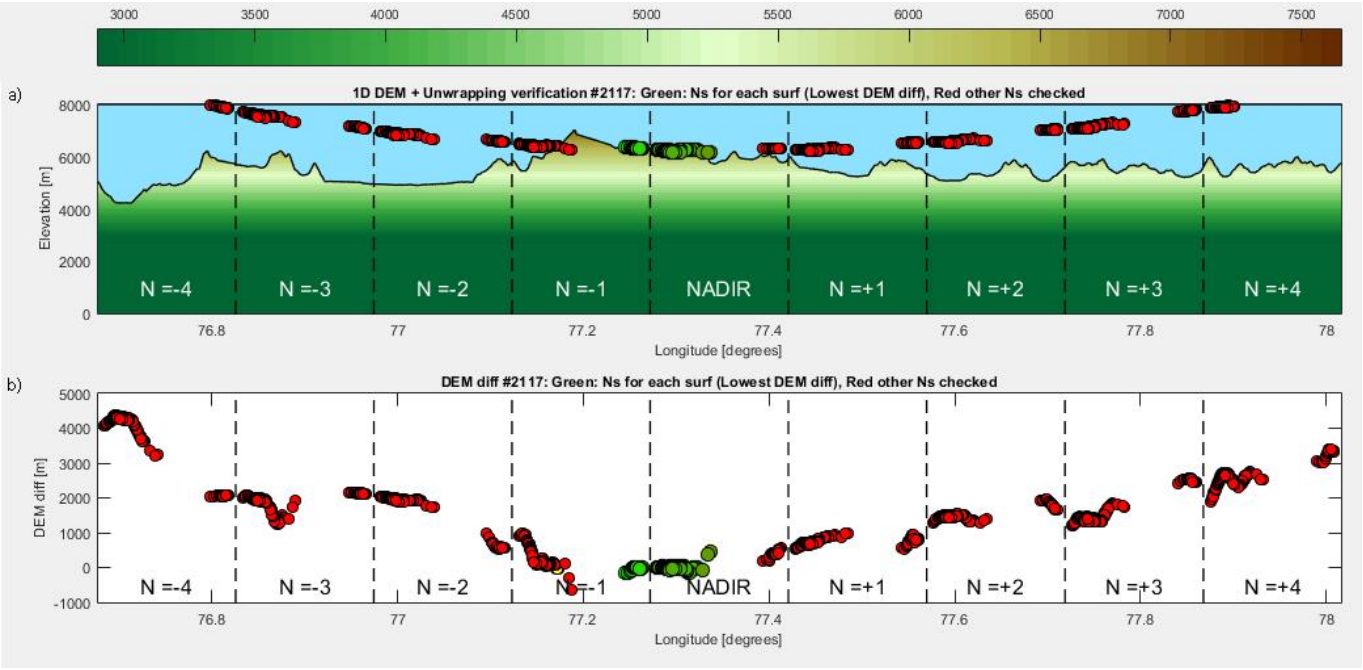

Figure 3: L2 Swath computation for the record 2117 of the L1b SIR_SIN_1B_20100717T194535 file. a) illustrates the comparison of the different elevations computed with the N=±4 . They are plotted in red against the DEM cross-section depicted with the colormap. b) shows the differences between the DEM and the elevations. The green bullets represent the elevations selected with the lowest difference and dispersion.

coverage improvement presented including the effect of the Ku band penetration to better estimate absolute accuracy of the method.

ACKNOWLEDGMENT

This work was supported by European Space Agency for the STSE CryoSat+ Mountain Glaciers (ESA/AO/1-8101/14/I-SBo), CryoSat+ MtG. The CryoSat-2 satellite altimetry data are freely available from their data access (https://earth.esa.int/web/guest/data-access). We are grateful to two anonymous reviewers and the editor, whose comments have significantly improved the manuscript.

TABLE I
DEM DIFF AND MAD RESULTS COMPARISON FOR EACH GLACIER

Glaciers	Length [km] / Orientation	conventional swath processing			Multi Swath processing			Improvement		
		#	DEM Diff [m]	MAD [m]	#	DEM Diff [m]	MAD [m]	%	DEM Diff [m]	MAD [m]
Aling	14.6 S	2328	11.46	27.78	2590	10.9	17.9	11%	0.56	9.88
Baltoro	54.7 W	106871	1.68	21.15	118136	1.96	15.28	11%	-0.28	5.87
Bilafond	17.4 S	4890	14.23	22.88	6990	12.38	14.69	**43%**	1.85	8.19
Braldu	22.3 N	6278	17.26	26.11	6647	15.82	23.37	6%	1.44	2.74
Chogolisa	14.8 W	15449	6.03	21.43	17455	2.06	14.72	13%	3.97	6.71
G076196E36156N	13.8 N	2337	15.49	36.87	3489	11.86	19.69	**49%**	3.63	**17.18**
G076520E35538N	6.34 W	2224	17.33	21.26	2581	16.14	14.66	16%	1.19	6.6
G076631E35901N	9.91 E	737	-13.18	37	846	-6.88	23.45	15%	6.3	**13.55**
G076811E35328N	7.0 W	6559	18.2	10.57	6426	16.69	8.88	-2%	1.51	1.69
G076875E35686N	25.0 NW	8779	-0.16	22.37	10096	0.06	15.27	15%	0.1	7.1
G077312E35560N	7.34 N	10177	22.56	24.09	11626	21.91	15.31	14%	0.65	8.78
Gasherbrum	20.7 NE	9604	-1.11	22.42	10589	-1.37	15.06	10%	-0.26	7.36
Ghandogoro	18.4 S	9488	9.12	20.83	10796	10.14	15	14%	-1.02	5.83
Masherbrum	10.5 SE	2279	92.31	36.94	3125	86.98	26.38	**37%**	5.33	**10.56**
Nagir	15.9 N	1572	10.52	22.5	2070	2.54	15.48	**32%**	7.98	7.02
North K2	12.2 N	6785	5.85	21.27	7006	6.55	15.46	3%	-0.7	5.81
North Terong	17.7 S	26273	13	17.01	31580	10.69	13.25	20%	2.31	3.76
Panmah	30.2 S	27268	4.71	23.1	31699	1.17	16.79	16%	3.54	6.31
Rimo	19.6 E	150440	11.03	17.4	157590	10.4	13.75	5%	0.63	3.65
Sherpikang	10.9 S	23249	11.06	15.77	24062	12.72	12.29	3%	-1.66	3.48
Siachen	62.8 SE	201606	8.44	17.9	223771	8.71	12.92	11%	-0.27	4.98
Siachin	33.5 S	39096	11.42	19.17	42068	9.73	13.85	8%	1.69	5.32
Singkhu	19.9 NW	11676	7.07	22.59	14406	6.01	17.45	23%	1.06	5.14
Sugatyanatjilga	33.9 E	70612	4.34	28.16	73717	5.41	18.77	4%	-1.07	9.39
Urbak	21.0 N	7891	-8.84	23.84	8224	-10.4	18.7	4%	-1.56	5.14
Yanatsugat	18.0 NE	13671	-5.02	26.41	16509	-1.79	17.8	21%	3.23	8.61
OVERALL		**768139**	**7.83**	**20.18**	**844094**	**7.57**	**14.69**	**10%**	**0.26**	**5.49**

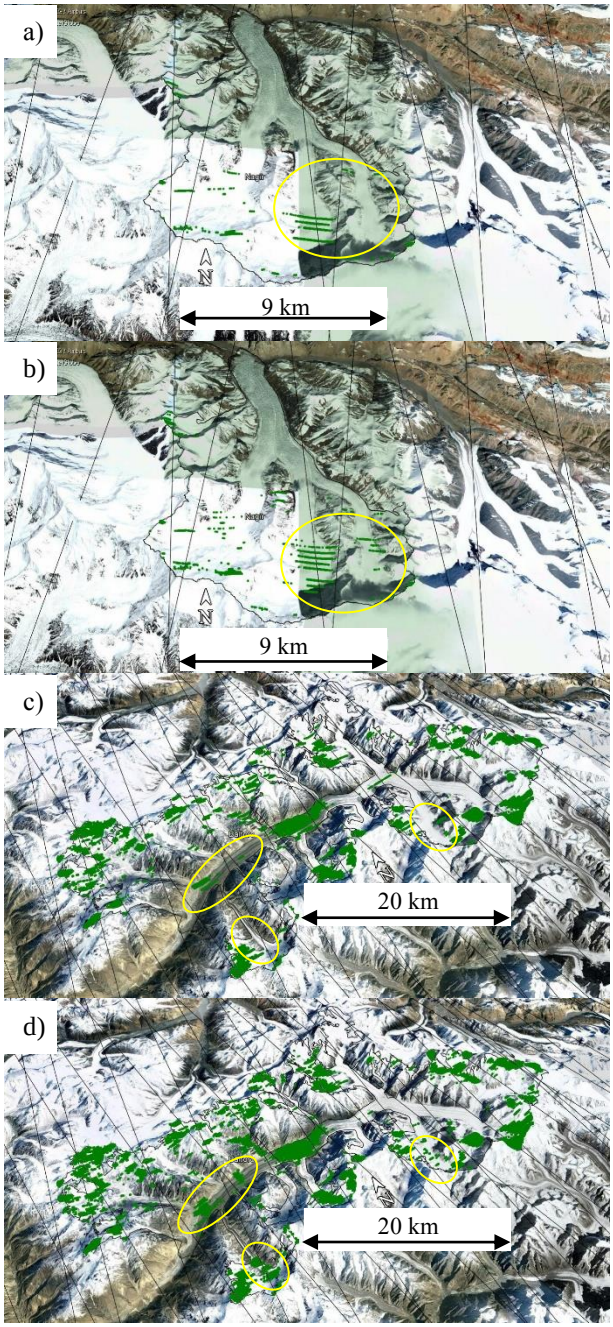

Figure 4. Elevations retrieved in the Nagir (top) and Baltoro glaciers (bottom) by the conventional processor, images a) and c), and the Multi Swath processor, images b) and d). The elevation measurements are depicted in green, the CryoSat-2 ground tracks in black and the main areas where the Multi Swath is improving the coverage are circled in yellow. Background image from CNES/ Airbus using Google Earth.

TABLE II
MULTI SWATH IMPROVEMENTS GROUPING GLACIERS BY ORIENTATION

Orientation	#	DEM Diff [m]	MAD [m]
North /South	188847	1.31	5.56
West / East	655247	0.07	4.26

REFERENCES

[1] Shepherd, A., Ivins, E.R., Geruo, A., Barletta, V.R., Bentley, M.J., Bettadpur, S., Briggs, K.H., Bromwich, D.H., Forsberg, R., Galin, N. and Horwath, M., 2012. A reconciled estimate of ice-sheet mass balance. Science, 338(6111), pp.1183-1189.

[2] Gardner, A.S., Moholdt, G., Cogley, J.G., Wouters, B., Arendt, A.A., Wahr, J., Berthier, E., Hock, R., Pfeffer, W.T., Kaser, G. and Ligtenberg, S.R., 2013. A reconciled estimate of glacier contributions to sea level rise: 2003 to 2009. Science, 340(6134), pp.852-857

[3] Kääb, A., Treichler, D., Nuth, C. and Berthier, E., 2015. Brief Communication: Contending estimates of 2003–2008 glacier mass balance over the Pamir–Karakoram–Himalaya. The Cryosphere, 9(2), pp.557-564.

[4] Gardelle, J., Berthier, E., Arnaud, Y. and Kaab, A., 2013. Region-wide glacier mass balances over the Pamir-Karakoram-Himalaya during 1999-2011 (vol 7, pg 1263, 2013). Cryosphere, 7(6), pp.1885-1886.

[5] Rankl, M. and Braun, M., 2016. Glacier elevation and mass changes over the central Karakoram region estimated from TanDEM-X and SRTM/X-SAR digital elevation models. Annals of Glaciology, 57(71), pp.273-281.

[6] Brun, F., Berthier, E., Wagnon, P., Kääb, A. and Treichler, D., 2017. A spatially resolved estimate of High Mountain Asia glacier mass balances from 2000 to 2016. Nature geoscience, 10(9), pp.668-673.

[7] Kääb, A., Berthier, E., Nuth, C., Gardelle, J. and Arnaud, Y., 2012. Contrasting patterns of early twenty-first-century glacier mass change in the Himalayas. Nature, 488(7412), p.495.

[8] Dehecq, A., Gourmelen, N., Shepherd, A., Cullen, R. and Trouvé, E., 2013, March. Evaluation of CryoSat-2 for height retrieval over the Himalayan range. In CryoSat-2 third user workshop.

[9] Screen, J.A. and Simmonds, I., 2010. The central role of diminishing sea ice in recent Arctic temperature amplification. Nature, 464(7293), p.1334.

[10] McMillan, M., Shepherd, A., Sundal, A., Briggs, K., Muir, A., Ridout, A., Hogg, A. and Wingham, D., 2014. Increased ice losses from Antarctica detected by CryoSat-2. Geophysical Research Letters, 41(11), pp.3899-3905.

[11] Foresta, L., Gourmelen, N., Pálsson, F., Nienow, P., Björnsson, H. and Shepherd, A., 2016. Surface elevation change and mass balance of Icelandic ice caps derived from swath mode CryoSat-2 altimetry. Geophysical Research Letters, 43(23).

[12] Gray, L., Burgess, D., Copland, L., Dunse, T., Langley, K., and Moholdt, G.: A revised calibration of the interferometric mode of the CryoSat-2 radar altimeter improves ice height and height change measurements in western Greenland, The Cryosphere, 11, 1041-1058, https://doi.org/10.5194/tc-11-1041-2017, 2017

[13] Gourmelen, N, Escorihuela, M, Shepherd, A, Foresta, L, Muir, A, Garcia-Mondejar, A, Roca, M, Baker, S & Drinkwater, MR 2017, 'CryoSat-2 swath interferometric altimetry for mapping ice elevation and elevation change' Advances in Space Research. DOI: 10.1016/j.asr.2017.11.014

[14] Gourmelen, N., Goldberg, D., Snow, K., Henley, S., Bingham, R., Kimura, S., Hogg, A., Shepherd, A., Mouginot, J., Lenearts, J., Ligtenberg, S. & van de Berg, W. 2017, "Channelized melting drives thinning under a rapidly melting Antarctic ice shelf", Geophysical Research Letters, 44, 9796–9804. 10.1002/2017GL074929.

[15] Cogley, G., Moelg, N.; Frey, H., Guo, W., Raup, B. H., Sakai, A., Liu, S., Nuimura, T., Paul, F., Bolch, T., 2015. GLIMS Glacier Database. Boulder, CO. National Snow and Ice Data Center. http://dx.doi.org/10.7265/N5V98602

[16] Steiner, J.F., Kraaijenbrink, P.D., Jiduc, S.G. and Immerzeel, W.W., 2018. Brief communication: The Khurdopin glacier surge revisited–extreme flow velocities and formation of a dammed lake in 2017. The Cryosphere, 12(1), p.95.